Bioorganic Chemistry 91 (2019) 103159

Contents lists available at ScienceDirect

Bioorganic Chemistry

journal homepage: www.elsevier.com/locate/bioorg

Design, synthesis, anticancer evaluation and docking studies of new pyrimidine derivatives as potent thymidylate synthase inhibitors

Lamia H.T. Amin[a], Taghreed Z. Shawer[a], Abeer M. El-Naggar[b,*], Hend M.A. El-Sehrawi[a]

[a] Department of Pharmaceutical Chemistry, Faculty of Pharmacy (girls), Al-Azhar University, Nasr City, Cairo, Egypt
[b] Department of Organic Chemistry, Faculty of Science, Ain Shams University, Abbassia, 11566 Cairo, Egypt

ARTICLE INFO

Keywords:
Anticancer
Thymidylate synthase
Pyrimidine
Docking
Apoptosis

ABSTRACT

Cancer is a perplexing and challenging problem for researchers. In this study, a series of 6-aryl-5-cyano-pyrimidine derivatives were designed, synthesized and evaluated for their anticancer activity against HePG-2, MCF-7 and HCT-116 cell lines. Compounds **2, 3d, 4a-c**, **5, 8** and **12** displayed high anticancer activity, comparable to that of 5-fluorouracil. Additionally, those compounds with effective anticancer activity were further assessed for their ability to inhibit thymidylate synthase (TS) enzyme. All the tested compounds demonstrated a marked TS inhibitory activity (33.66–74.98%), with IC_{50} ranging from 3.89 to 15.74 nM. Moreover, apoptosis studies were conducted on the most potent compound **8**, to evaluate its proapoptotic potential. Interestingly, compound **8** induced the level of active caspase 3, and elevated the Bax/Bcl2 ratio 44 folds in comparison to the control. Finally, a molecular docking study was conducted to detect the probable interaction between the active compounds and the thymidylate synthase active site.

1. Introduction

Cancer remains one of the most menacing diseases in the world [1]. It is considered the second cause of death after cardiac diseases [2]. Liver cancer is the second most common cancer death causes worldwide [3], while colorectal cancer is the fourth one [4]. Abnormalities in the genetic material are the causes of the various cancer types [5]. One of the important approach to treat the uncontrolled cell division and growth manifested by the cancer cells is to use drug capable of interfering with the synthesis of the nucleic acids DNA/RNA, and inhibiting their normal function [6,7]. Thymidylate synthase (TS) catalyzes the reductive methylation of 2′-deoxyuridine-5′-monophosphate (dUMP) to 2-deoxythymidine-5-monophosphate (dUMP), a DNA building unit, assisted by the cofactor N5,N10-methylenetetrahydrofolate (MTHF) [8–10]. Human TS (hTS) is an essential enzyme for DNA replication, thus it is considered an interesting target for the development of anticancer treatments. Human TS (hTS) exists in the equilibrium of active and inactive conformations [11]. TS plays an important role in the synthesis of key proteins that regulate apoptosis [12]. Inhibition of TS was reported to induce apoptosis.

An example of drugs inhibiting TS enzyme is 5-fluorouracil, the drug of choice for metastatic colorectal cancer with 25% positive patient's response [13]. 5-Fluorouracil (5-FU) is an analogue of uracil with fluorine atom replacing hydrogen at the C-5 position. It was one of the first rationally designed, synthesized anticancer drugs. 5-FU is converted to 5-fluorodeoxyuridine monophosphate (FdUMP) which forms a stable ternary complex with thymidylate synthase and the cofactor N5,10-methylenetetrahydrofolate [14–16]. 5-FU remains covalently and irreversibly bound to the active site, misincorporated into RNA, disrupting its function and blocking the synthesis of thymidine leading to DNA damage [1,9,14]. Therefore, targeting TS and its inhibition in TS over expressing cells as tumor cells, have become a major goal in cancer chemotherapy treatment [16]. Herein we provide an approach to explore and expand the anticancer activity of synthesized series of pyrimidine derivatives, via the structural modifications (Fig. 1), of the promising lead compound **A** which showed a potent anticancer activity against HepG2 cell line with IC_{50} value of 28 μM [17]. Our rational design is founded on structural diversification of compound A through conserving the cyanopyrimidine group, while simplification at position 4 and substitution at position 2 with different moieties, to attain an active anticancer agent with an improved activity and selectivity towards cancerous cells. The newly synthesized compounds were evaluated for their anticancer activity against three cell lines; HepG2, HCT-116 and MCF-7. Moreover, the most active compounds were tested for inhibition of thymidylate synthase (TS) enzyme, and their IC_{50} values were evaluated in addition to the apoptosis induction potential of the compounds. Finally, a molecular docking study was performed to explore the probable interaction of the tested compounds with

* Corresponding author at: Chemistry Department, Faculty of Science, Ain Shams University, Abbassia, 11566 Cairo, Egypt.
E-mail address: elsayedam@sci.asu.edu.eg (A.M. El-Naggar).

https://doi.org/10.1016/j.bioorg.2019.103159
Received 9 December 2018; Received in revised form 25 June 2019; Accepted 25 July 2019
Available online 29 July 2019
0045-2068/

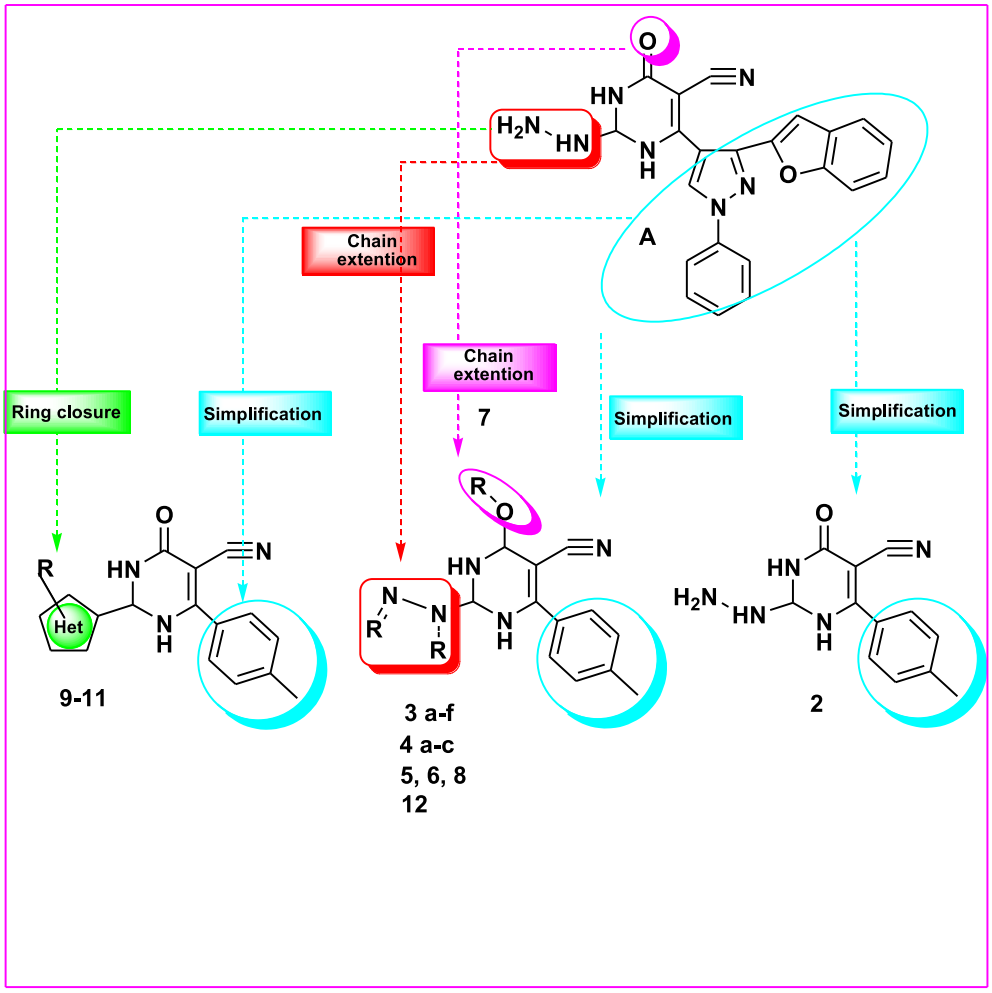

Fig. 1. Structure-based design of cyanopyrimidine derivatives via modification of lead compound **A**.

thymidylate synthase enzyme.

2. Results and discussion

2.1. Chemistry

In connection with our program [18–20], we aim to design and synthesize a novel series of biologically active cyanopyrimidine derivatives to evaluate their anticancer activity. Thus, the sequence of reactions used in the synthesis of the title compounds is shown (Schemes 1–3). The starting key compound **1** was synthesized via one-pot cyclocondensation reaction, in which, equivalent molar quantities of aromatic aldehydes, ethyl cyanoacetate and thiourea were allowed to react in absolute ethanol in presence of anhydrous K_2CO_3, then neutralized with acetic acid [21,22]. Treating the thiol derivative **1** with hydrazine hydrate by refluxing in absolute ethanol afforded

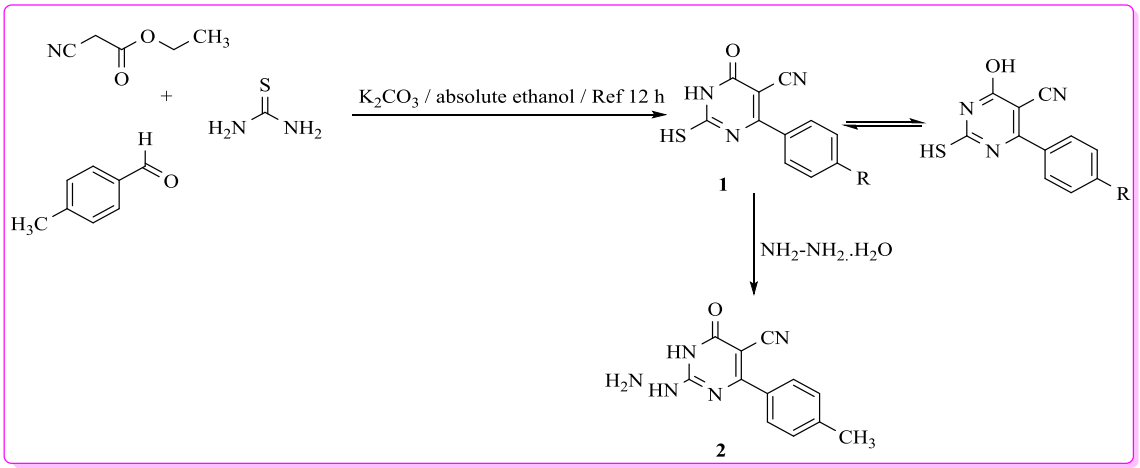

Scheme 1. General procedure for synthesis of target compound **2**.

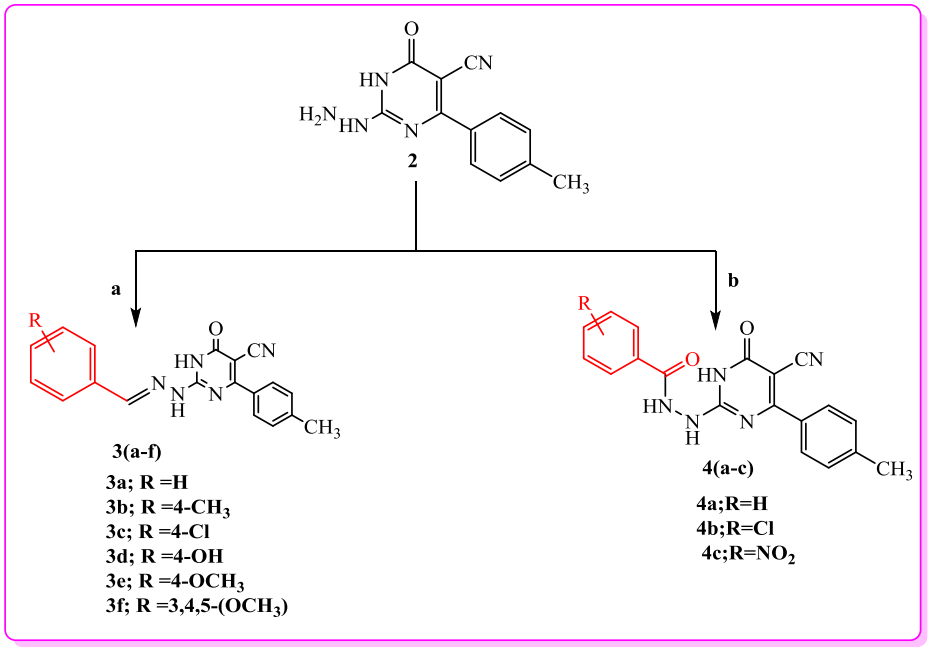

Scheme 2. Reagents and conditions: (a) appropriate aromatic aldehyde, ethanol, reflux. (b) substituted benzoyl chloride, TEA, dioxane, reflux.

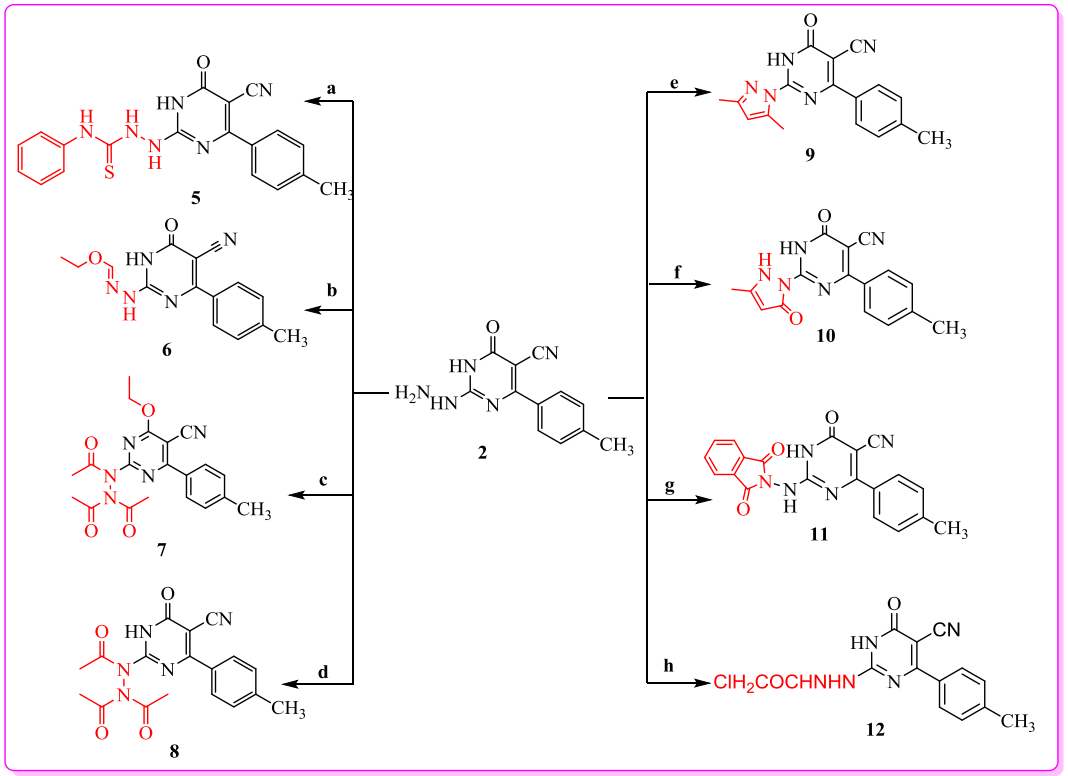

Scheme 3. Reagents and conditions: (a) phenyl isothiocyanate, pyridine, reflux. (b) TEOF (0.01 mol), AC_2O 10 mL, reflux. (c) TEOF, 5 mL/AC_2O, 5 mL reflux. (d) AC_2O, reflux. (e) Acetylacetone, glacial acetic acid , reflux. (f) Ethyl acetoacetate, ACOH, reflux. (g) Phthalic anhydride, glacial acetic acid, reflux. (h) $ClCH_2COCl$, dioxane, reflux.

hydrazinoyl **2** (Scheme 1).

Moreover, we studied the nucleophilicity of NH_2 to form Schiff bases through reaction of 2-hydrazinyl-1,6-dihydro-6-oxo-4-ptolylpyrimidine-5-carbonitrile **2,** with substituted aromatic aldehydes namely benzaldehyde, tolualdehyde, 4-chloroaldehyde, 4- hydroxyl aldehyde, 4-methxyaldehyde and 3,4,5 trimethoxybenzaldehyde. The reaction of the former components in absolute ethanol produced the corresponding target compounds **3a-f**, respectively (Scheme 2).

The structure of compounds **3a-f** were characterized by spectroscopic tools The I.R showed the presence of bands between 3200 and 3400 and 1680–1685 cm^{-1} for the amide groups NH and C=O groups, respectively. Moreover, ^1H NMR spectra for this group exhibited a singlet corresponding to the imine proton (CH = N) at the range 8.07–8.17 ppm denoting the formation of the Schiff's base. Furthermore

the MS spectrum of a showed the molecular ion peak confirmed the structures (c.f. experimental).

Refluxing equimolar amount of compound **2** and the substituted benzoyl chloride namely, benzoylchloride, 4-chlorobenzoyl chloride and 4-nitrobenzoylchloride in dioxane and TEA as catalyst, afforded the target compounds **4a-c,** respectively (Scheme 2). IR spectra for this series were in agreement with the predicted structures as they showed the disappearance of NH_2 bands and presence of characteristic absorption bands of carbonyl groups around 1634, 1662 cm^{-1}. In addition, ^1H NMR spectra revealed an increase in the number of aromatic protons. The structure **4a-c** is forthcoming from the study of ^1H NMR and mass spectra.

Finally, Compound **2** was condensed with different electrophiles namely, phenyl isothiocyanate, triethylorthoformate, acetic anhydride, acetylacetone, ethylacetoacetate, phthalic anhydride and chloroacetyl chloride to afford the title compounds **5–12** respectively (Scheme 3). The suggested mechanisms for formation of the structures of compounds **6** and **7** were in Supplementary Data.

The structures of all newly prepared compounds were confirmed by spectral and elemental analyses, which were in full agreement with the proposed structures.

2.2. Biological evaluation

2.2.1. In vitro cytotoxic activity

The in vitro anticancer activity of the eighteen newly synthesized compounds was evaluated against three cell lines, namely; the liver cancer cell line (HepG2), the colon cancer cell line (HCT-116) and the breast cancer cell line (MCF-7). 5-Fluorouracil was used as a reference standard and showed IC_{50} values of 60.73, 40.74 and 41.51 μM for the three cell lines respectively. The results were expressed as IC_{50} values and listed in (Table 1). The anticancer results profile suggested that, test compounds showed variable activity compared to the reference drug. The anticancer data revealed that compounds **2, 3d, 4a-c**, **5** and **12,** possessed a remarkable anticancer activity. Compound **2** displayed 2 and 1.7 folds the activity of 5-Fu against HepG2 (IC_{50} = 31.08 μM) and HCT-116 cell lines (IC_{50} = 23.62 μM) respectively, and was equipotent to the reference drug against MCF-7 cell line (IC_{50} = 38.13 μM), while compound **3d** displayed 1.7, 1.3 and 1.2 folds the activity of 5-Fu with IC_{50} values of 36.19, 31.56 and 35.32 μM against HepG2, HCT-116 and MCF-7 cell lines respectively. Compound **4a** was more potent than the reference drug against HepG2 (IC_{50} = 45.57 μM), MCF-7(IC_{50} = 24.90 μM), and equipotent against HCT-116 cell line (IC_{50} = 40.07 μM) while compound **4b** displayed 2.4, 1.7 and 1.1 folds the activity of 5-Fu with IC_{50} values of 25.03, 23.14 and 36.70 against the three cell lines respectively. **4c** Demonstrated 1.7 fold the activity of 5-Fu, with IC_{50} values of 32.94, 23.00 and 23.49 μM for the three cell lines respectively. Moreover**,** Compound **5** exhibited 3, 1.6 and 2.2 folds the activity of 5-Fu with IC_{50} values of 21.15, 24.97 and 19.12 μM against the three cell lines respectively. Compound **12** was equipotent to the reference drug with IC_{50} values of 59.48, 41.54 and 38.39 μM against HepG2, HCT-116 and MCF-7 cell lines respectively. Compounds **11** was equipotent to the reference drug against HepG2 cell line, while compounds **8** was equipotent to the reference drug against MCF-7cell line, but showed good activities against other tested cell lines. Compounds **3a, b** and **9** possessed a moderate to weak anticancer activity.

Table 1
In vitro anti-proliferative activities towards HePG-2, HCT-116 and MCF-7 cell lines and thymidylate synthase (TS).

Comp.	IC_{50} (μM)[a]			IC_{50} (nM)[a]	TS inhibition %
	HepG2	HCT-116	MCF-7	TS	
2	31.08	23.62	38.13	4.42	69.08
3a	189.45	143	98.97	NT[b]	NT[b]
3b	206.18	211.71	188.42	NT[b]	NT[b]
3c	216.32	235.89	189.38	NT[b]	NT[b]
3d	36.19	31.56	35.32	13.05	48.31
3e	264.34	247.09	223.99	NT[b]	NT[b]
3f	87.97	65.56	49.35	NT[b]	NT[b]
4a	45.57	40.07	24.90	15.74	33.66
4b	25.03	23.14	36.70	4.72	67.23
4c	32.94	23.00	23.49	4.21	74.24
5	21.51	24.97	19.12	4.63	67.06
6	187.11	226.16	212.30	NT[b]	NT[b]
7	191.62	235.30	260.23	NT[b]	NT[b]
8	63.42	50.35	36.47	3.89	70.41
9	142.76	118.92	153.73	NT[b]	NT[b]
10	213.49	152.06	181.77	NT[b]	NT[b]
11	49.87	47.09	72.19	NT[b]	NT[b]
12	59.48	41.54	38.39	8.13	64.18
5-FU	38.44	40.74	41.51	——	——
Dasatinib				2.94	72.25

[a] IC_{50} values are the mean ± S.D. of three separate experiments.
[b] NT: Compounds not tested.

2.2.2. In vitro assay of thymidylate synthase (TS) activity

The most active compounds in cytotoxic assay (**2**, **3_d**, **4_{a-c}**, **5**, **8** and **12**) were further evaluated to determine their inhibitory activities against thymidylate synthase (TS) aiming to recognize the probable anticancer activity mechanism of action of these compounds. The activity of TS was measured spectrophotometrically according to reported method [23]. Dasatinib was used as a positive control in this assay [24,25]. The results were reported as enzymatic inhibition percentage (%) and a 50% inhibition concentration value (IC_{50}) (Table 1).

The tested compounds showed good inhibitory activity with IC_{50} values ranging from 3.89 to 15.74 nM, which were consistent with that of their in vitro anticancer activities. Dasatinib as a reference compound showed 72.25% TS inhibition. Compounds **4c** and **8** showed potent inhibitions more than 74% for the TS activity with IC_{50} values of 4.21 and 3.89 nM, respectively. Good inhibitions also exhibited by compounds **2**, **4b** and **5,** at low IC_{50} values of 4.42, 4.72 and 4.63 nM, respectively. Moreover, compounds **3d** and **12** displayed moderate inhibitions above 67% with IC_{50} values of 13.05 and 8.13 nM, respectively.

2.2.3. Apoptosis studies

As previously mentioned, the regulatory role of TS may be implicated in the synthesis of different proteins that regulate apoptosis [11]. As our synthesized compounds successfully inhibited TS enzyme, then expectedly they will induce apoptosis. Their potential to induce apoptosis was determined by monitoring the levels of active caspase 3 and the Bax/Bcl2 ratio that presents proof for induction of apoptosis.

2.2.3.1. Effects on the level of active caspase-3. The investigation of Caspase 3 expression level indicates apoptosis induction. In the present study, HepG2 cells were treated with the most active TS inhibitor **8** with IC_{50} in the nanomolar range (IC_{50} 3.89 nM). Results revealed that compound **8** upregulated the caspase 3 level 7.3 folds as compared to the control, thus proving compound **8** apoptosis induction potential.

2.2.3.2. Effects on mitochondrial apoptosis pathway proteins Bax and Bcl-2. Bcl2 and Bax are members of Bcl-2 family of proteins that are responsible for syncing the mitochondrial apoptotic pathway. Bcl2 and Bax tune this programmed process as Bcl2 suppresses apoptosis whereas Bax induces it. Consequently, the balance between these two proteins is judgmental for the cell potential to undergo apoptosis. In this study, HepG2 cells were treated with compound **8** and its effect on Bcl2 and Bax was quantified as showed in (Table 2, Fig. 2). Results revealed that compound **8** reduced the level of the antiapoptotic protein Bcl2 by 7.5 folds as compared to the control while it elevated the level of the pro-apoptotic protein Bax by 5.9 folds. The ratio between Bax and Bcl2 was also calculated as a more decisive parameter. The Bax/Bcl2 ratio for compound **8** was calculated to be 44 folds as compared to the

Table 2
Effect of compound **8** on the genes expression of some apoptosis key markers.

Comp. No	Caspase 3 Pg/ml	BAX IU/ml	BCL2 IU/ml
8	7.319186	0.133773	5.938101
Control	6.015439	0.152966	7.814144

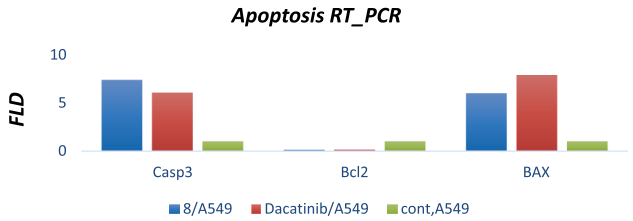

Fig. 2. Effect of compound **8** on the genes expression of some apoptosis key markers.

control, confirming that the compound shifted the cells towards undergoing apoptosis.

2.3. Molecular docking

To understand the obtained biological data on a structural basis, the most active compounds were evaluated through the molecular docking studies using Molecular Operating Environment (MOE) version 2014, 0901. The enzyme structure was prepared through removal of water molecules and restoration of missing hydrogen atoms.

In the present investigation, the 3D-coordinates in X-ray crystal structure of Human Thymidylate Synthase (PDB code 6QXG) was used as the receptor model in the docking simulation to predict the binding modes, affinities and orientation at the active site of the enzyme (Table 3). The inhibitors are held in the active pocket by combination of various interactions [26]. From the published literatures, Arg50, Ser216, Asn226 and Asp218 are the essential amino acids involved in the interaction with enzyme inhibitors [27,28] (see Table 4).

The proposed binding mode of FdUMP showed an affinity value of −4.52 kcal/ mol. The phosphate group was involved in five hydrogen bonding interactions with Arg50 and Arg215. The oxygen atom formed two hydrogen bond with side chain of His256 and TYR 258. Finally, the two-keto groups formed two hydrogen bonds with Asp218 and Asn226 (Figs. 3 and 4). (Table 3).

Overall, it was found that most of the studied compounds are expected to have the same binding mode of FdUMP (Table 3).

The proposed binding mode of compound **8** showed affinity value of −5.39 Kcal/mol. It formed 4 hydrogen bonds, one of them between acetyl group oxygen and Asn226. pyrimidinone oxygen was anchored by two hydrogen bonds interactions with Asp218 and Gly222. The last one between cyano group at the 5-position of pyrimidine moiety and Ser216 (Figs. 5 and 6).

2.3.1. Structure activity relationships (SAR)

The introduction of the hydrazide, **2** or benzohydrazide, **4a-c** moieties in position 2 of the pyrimidine scaffold lead to a marked increase in the anticancer activity. However, p-chloro or p-nitro substituted derivatives **4b, c** showed higher anticancer activity than its unsubstituted counterpart **4a**. This indicates that para substitution with electron withdrawing group might have a positive impact on the activity with respect to the unsubstituted derivative. The incorporation of 4-hydroxy benzylidene **3d** to the hydrazide group gave a potent anticancer activity than the other counterparts **3a-c, 3e**, but still less than its starting compound which contain the hydrazide moiety **2**. The presence of phenylthiosemicarbazide moiety **5** instead of the hydrazide moiety resulted in superior anticancer activity as compared to all newly synthesized compounds.

Table 4
Crystal and experimental data for the compound **7**.

Parameter	Result
Empirical formula	$C_{20}H_{21}N_5O_4$
Formula weight (g mol^{-1})	M_r = 395.419
Temperature	T = 298 K
Crystal system	Monoclinic
Space group	C2/c
a (Å)	26.6973 (9)
b (Å)	11.3330 (4)
c (Å)	15.2601 (5)
α (deg)	90.00°
β (deg)	116.517 (2)°
ϒ (deg)	90.00°
V $Å^3$	4131.4 (2)
Z	8
Dx	1.272 Mg m^{-3}
radiation	Mo K_α radiation (λ = 0.71073)
μ	0.091
Colour	Colourless

3. Conclusion

A new series of 6-aryl-5-cyano- pyrimidine derivatives were synthesized and evaluated for their anticancer activity against HePG-2, MCF-7 and HCT-116 cell lines. The thymidylate synthase inhibitory activity of the most active compounds was recorded. The results revealed that compound **8** showed a potent anticancer activity with high TS inhibitory activity, its IC_{50} value was 3.89 nM. The proapoptotic potential of our compounds was evaluated via Apoptosis studies for compound **8**. Results showed that compound **8** boosted the level of active caspase 3 by 7.3 folds as compared to the control. Additionally, the Bax/Bcl2 ratio of compound **8** was calculated and was found to be 44 folds in comparison to the control.

4. Experimental section

4.1. Chemistry

4.1.1. General

All melting points were measured on a Gallen Kamp melting point apparatus (Sanyo Gallen Kamp, UK) and were uncorrected. The Microwave reactions were done by Microsynth instrument type MA143 (Micro wave flux). The IR spectra were recorded on a Pye-Unicam SP-3-300 infrared spectrophotometer (KBr dicks) and expressed in wave number (cm^{-1}). ^{1}H NMR spectra were run at 300 and 400 MHz, on a Varian Mercury VX-300 and Bruker Avance III NMR spectrometer respectively. The mass spectra were recorded on Shimadzu GCMS-QP-

Table 3
The docking energy scores of the most active compound with the amino acid residues in the binding site of TS.

Cpd. No.	Docking score (Kcal/mol)	No. of H-bonds	Amino acid residues (bond length A°)
FdUMP	−4.52	9	Asn 226 (2.78), Asp 218 (2.74), His 256 (2.74), Tyr 258 (2.83), Arg 50 (3.09), Arg 50 (2.82), Arg 215 (3.40), Arg 215 (2.81), Arg 215 (2.89)
8	−5.39	4	Asp 218 (3.32), Gly222 (3.46), Ser216 (3.08), Asn 226 (3.25)

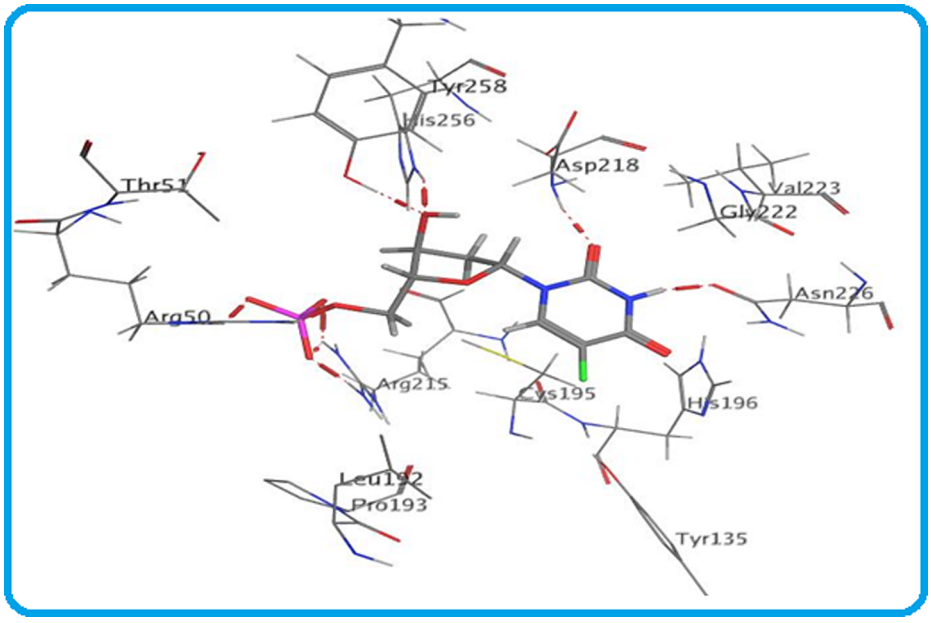

Fig. 3. Predicted binding mode of FdUMP at the TS binding site 3D.

1000EX mass spectrometer at 70 eV. Elemental analyses were performed on CHN analyzer and all compounds were within ± 0.4 of the theoretical values. The reactions were monitored by thin-layer chromatography (TLC) using TLC sheets coated with UV fluorescent silica gel Merck 60 F254 plates and were visualized using UV lamp and different solvents as mobile phases. All reagents and solvents were purified and dried by standard techniques. Compounds **1** [21,22,29] was previously reported.

4.1.2. Synthesis of 2-hydrazinyl-1,6-dihydro-6-oxo-4-p-tolyl pyrimidine-5-carbonitrile (2)

A mixture of **1** (10 mmol) and hydrazinehydrate 99% (20 mmol) was refluxed in absolute (30 mL) ethanol for 10 h. the formed solid was filtered off, dried and recrystallized from ethanol afforded compound **2**.

Yield 65%; yellow crystal; m.p. 234–236 °C (EtOH); IR (cm^{-1}): br 3325, 3289 (NH, NH_2), 3032 (CH-aromatic), 2947 (CH-aliphatic), 2207 (CN), 1665 (CO) amid; ^{1}H NMR (400 MHz, DMSO-d_6) δ (ppm): 2.35 (s, 3H, CH_3), 7.28 (d, 2H, Ar-H, J = 8 Hz), 7.66 (d, 2H, Ar-H, J = 8 Hz), 8.19 (s, 1H, NH_2, D_2O exchangeable), 10.15 (s, 1H, NH_2, D_2O exchangeable); MS (m/z): 241.12 (M^+, 100%). Anal. Calcd for $C_{12}H_{11}N_5O$ (371.41): C, 59.74; H, 4.60; N, 29.03; Found: C, 59.74; H, 4.60; N, 29.03%.

4.1.3. General procedure for synthesis of 2-(2-benzylidenehydrazinyl)-6-oxo-4-(p-tolyl)-1,6-dihydropyrimi-dine-5-carbonitrile (3a-f)

A mixture of compound **2** (10 mmol) and the appropriate aromatic aldehyde (10 mmol) namely, benzaldehyde, tolualdehyde, 4-chlorobenzaldehyde, 4-hydroxybenz-aldehyde, 4-methoxybenzaldehyde and 3,4,5-trimethoxybenzaldhyde in ethanol (50 mL) was heated under reflux for about 8–10 h. The solid obtained was filtered off dried and recrystallized from methanol to give the corresponding title compounds ***(3a-f)***, respectively.

4.1.3.1. 2-(2-benzylidenehydrazinyl)-6-oxo-4-(p-tolyl)-1,6-dihydropyrimidine-5-carbonitrile (3a). Yield 73%; yellow crystal; m.p over 300° C (MeOH); IR (cm^{-1}): 3143 (NH), 3046 (CH-aromatic), 2921 (CH aliphatic), 2208 (CN), 1675 (CO);^{1}H NMR (400 MHz, DMSO-d_6) δ (ppm): 2.37 (s, 3H, CH_3),7.33 (d, 2H, Ar-H), 7.42 (d, 2H, Ar-H),

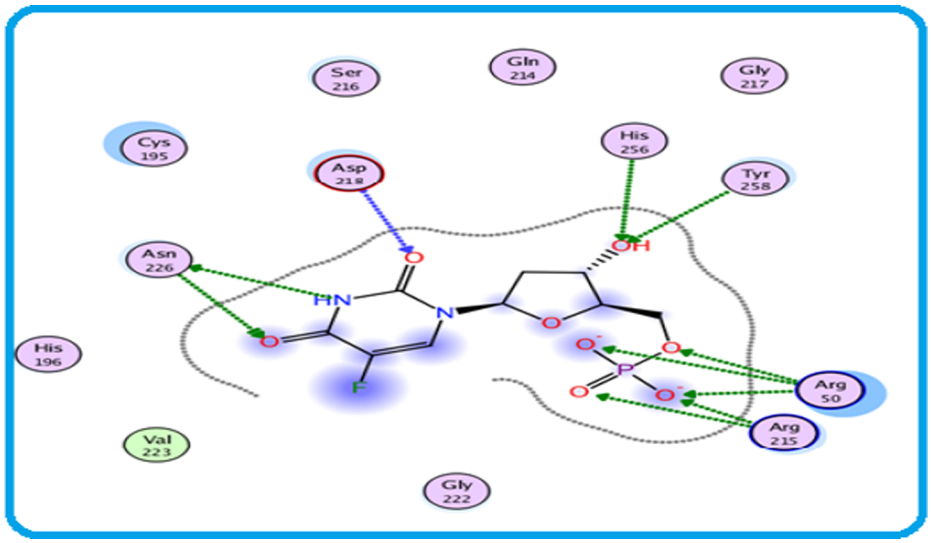

Fig. 4. Predicted binding mode of FdUMP at the TS binding site 2D.

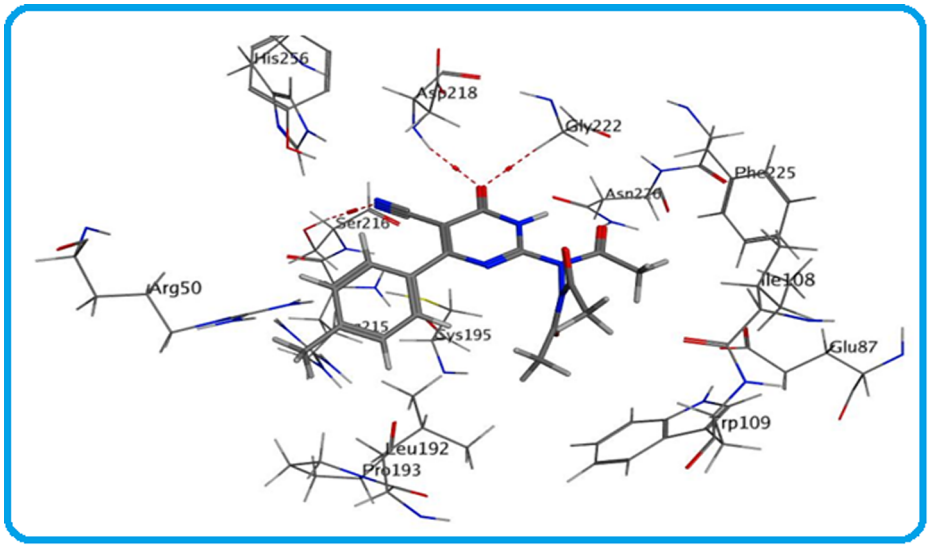

Fig. 5. Predicted binding mode of compound **8** at the binding site of TS.

7.98–8.01 (m, 3H, Ar-H of phenyl ring), 7.77 (d, 2H, Ar-H of phenyl ring), 7.98–8.01 (m, 3H, Ar-H of phenyl ring), 8.17 (s, 1H, N = CH), 12.37 (s, 2H, 2NH, D_2O exchangeable); MS (*m/z*) (%) 329.15 (M^+, 77.21), 90.06 (100). Anal. Calcd for $C_{19}H_{15}N_5O$ (329.36): C, 69.29; H, 4.59; N, 21.26; Found: C, 69.29; H, 4.59; N, 21.26%.

4.1.3.2. 2-(2-(4-methylbenzylidene)hydrazinyl)-6-oxo-4-(p-tolyl)-1,6-dihydropyrim idine-5-carbonitrile (3b). Yield 81%; yellow crystal; m.p. over 300 °C (MeOH); IR (cm^{-1}): 3194 (NH), 3030 (CH-aromatic), 2917 (CH aliphatic), 2208 (CN), 1664 (CO); ^1H NMR (400 MHz, DMSO-d_6) δ (ppm): 2.33 (s, 3H, CH_3), 2.37 (s, 3H, CH_3), 7.23 (d, 2H, Ar-H, J = 8 Hz,), 7.33 (d, 2H, Ar-H, J = 8 Hz), 7.76 (d, 2H, Ar-H, of benzylidene ring, J = 8 Hz), 7.88 (d, 2H, Ar-H, of benzylidene ring, J = 8 Hz), 8.13 (s, 1H, N = CH): 12.32 (s, 2H, 2NH, D_2O exchangeable); MS (*m/z %*): 343.15 (M^+,42.03), 184.09 (100); Anal. Calcd for $C_{20}H_{17}N_5O$ (343.39): C, 69.96; H, 4.99; N, 20.40; Found: C, 69.96; H, 4.99; N, 20.40%.

4.1.3.3. 2-(2-(4-chlorobenzylidene)hydrazinyl)-6-oxo-4-(p-tolyl)-1,6-dihydropyrimidine -5-carbonitrile (3c). Yield 70%; yellow crystal; m.p. 300–302 °C (MeOH); IR (cm^{-1}): br 3229, 3175 (NH), 3048 (CH aromatic), 2204 (CN), 1656 (CO); ^1H NMR (400 MHz, DMSO-d_6) δ (ppm): 2.37 (s, 3H, CH_3), 7.23 (d, 2H, Ar-H), 7.33 (d, 2H, Ar-H), 7.75 (d, 2H, Ar-H of benzylidene ring), 7.88 (d, 2H, Ar-H of benzylidene ring), 8.13 (s, 1H, N = CH): 12.59 (s, 2H, 2NH, D_2O exchangeable); MS *m/z* (%) 365.10 (M^{+2}.17.79), 363.11 (M^+. 52.14), 89.08 (100); Anal. Calcd for $C_{19}H_{14}ClN_5O$ (363.81): C, 62.73; H, 3.88; 19.25; Found: C, 62.73; H, 3.88; N, 19.25%.

4.1.3.4. 2-(2-(4-hydroxybenzylidene)hydrazinyl)-6-oxo-4-(p-tolyl)-1,6-dihydropyrimidine-5-carbonitrile (3d). Yield 89%; yellow crystal; m.p. over 300 °C (MeOH); IR (cm^{-1}): 3478 (OH), 3394, 3160 (2NH), 3062 (CH Aromatic), 2206 (CN), 1673 (CO); ^1H NMR (400 MHz, DMSO-d_6) δ (ppm): 2.37 (s, 3H, CH_3), 6.79 (d, 2H, Ar- H of benzylidene ring), 7.32 (d, 2H, Ar-H), 7.76 (d, 2H, Ar- H), 7.81 (d, 2H, Ar-H of benzylidene ring), 8.07 (s, 1H.N = CH): 9.87 (s, 1H, OH, D_2O exchangeable), 12.13 (s, 2H, 2NH, D_2O exchangeable); MS: *m/z*(%) 345.12 (M^+, 39.75%), 40.17 (100); Anal. Calcd for $C_{19}H_{15}N_5O2$ (345.36): C, 66.08; H, 4.38; N,

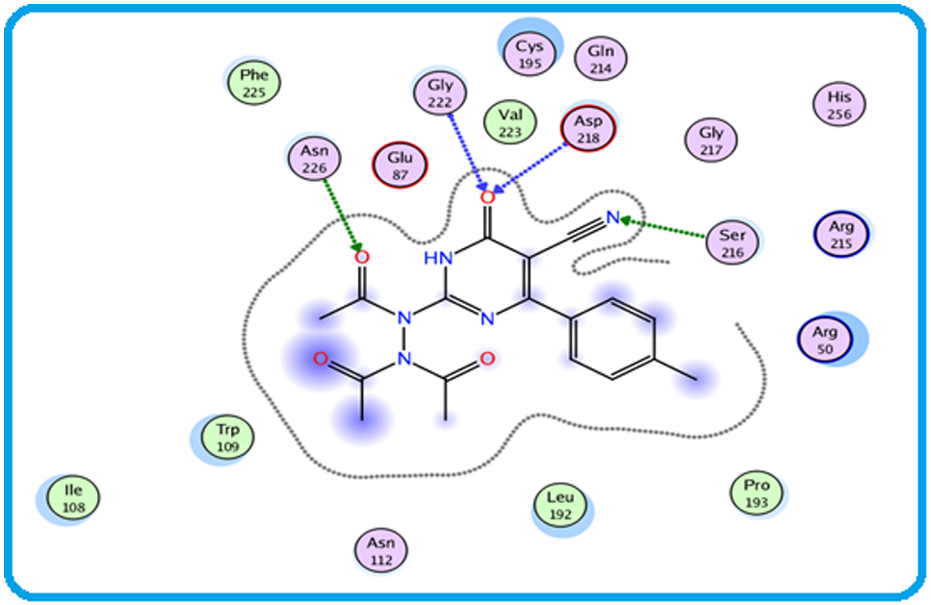

Fig. 6. Mapping surface showing compound **8** occupying the active pocket of TS.

20.28; Found: C, 66.08; H, 4.38; N, 20.28%.

4.1.3.5. 2-(2-(4-methoxybenzylidene) hydrazinyl)-6-oxo-4-(p-tolyl)-1,6-dihydropyrimidine-5-carbonitrile (3e). Yield 83%; yellow crystal; m.p. 335–337 °C (MeOH); IR (cm^{-1}): 3209, 3160 (NH), 3041 (CH-aromatic), 2925 (CH-aliphatic), 2213 (CN), 1662 (CO); ^{1}H NMR (400 MHz, DMSO-d_6) δ (ppm): 2.37 (s, 3H, CH_3), 3.79 (s, 3H, OCH_3), 6.97 (2H, d, Ar-H, J = 8 Hz), 7.32 (2H, d, Ar-H, J = 8 Hz), 7.75 (2H, d, Ar-H, J = 8 Hz), 7.94 (d, 2H, Ar-H, J = 8 Hz), 7.97 (s, 1H, NH, D_2O exchangeable), 7.24 (s, 1H, NH, D_2O exchangeable), 10.15 (d, 2H, NH_2, D_2O exchangeable); MS (m/z): 359.14 (M^+, 52.20%), 198.12 (100%). Anal. Calcd for $C_{20}H_{17}N_5O_2$ (359.39): C, 66.84; H, 4.77; N, 19.49; Found: C, 66.84; H, 4.77; N, 19.49%.

4.1.3.6. 6-oxo-4-(p-tolyl)-2-(2-(2,4,6-trimethoxybenzylidene)hydrazinyl)-1,6-dihydro pyrimidine-5-carbonitrile (3f). Yield 88%; yellow crystal; m.p. over 300 °C (MeOH); IR (cm^{-1}): 3411, 3214 (2NH), 3042 (CH aromatic), 2219 (CN), 1672 (CO); ^{1}H NMR (400 MHz, DMSO-d_6) δ (ppm): 2.37 (s, 3H, CH_3), 3.26 (s, 3H, OCH_3), 3.66 (s, 3H, OCH_3), 3.69 (s, 3H, OCH_3), 7.22 (s, 2H, Ar- H of benzylidene ring), 7.31 (d, 2H, Ar-H), 7.73 (d, 2H, A-H),8.07 (s.1H.N = CH), 12.08 (s, 1H, NH, D_2O exchangeable), 12.50 (s, 1H, NH, D_2O exchangeable); MS m/z (%): 419.15 (60.94), 193.07 (100); Anal. Calcd for $C_{22}H_{21}N_5O_4$ (419.43): C, 63.00; H, 5.05; N, 16.70%; Found: C, 63.00; H, 5.05; N, 16.70%.

4.1.4. General procedure for synthesis of N'-(5-cyano-1,6-dihydro-6-oxo-4-p-tolylpyrimidin-2-yl)-4-substituted benzohydrazide (4a-c)

A mixture of compound **2** (10 mmol), substituted benzoyl chloride (10 mmol), with a catalytic amount of triethylamine was refluxed in dry dioxane for 10 h. The reaction mixture was cooled and then poured over ice water acidified with hydrochloric acid. The precipitate formed was filtered, dried, and recrystallized from dioxane afforded compounds ***(4a-c)***.

4.1.4.1. N'-(5-cyano-1,6-dihydro-6-oxo-4-p-tolylpyrimidin-2-yl) benzohydrazide (4a). Yield 69%; yellow crystal; m.p. 221–223 °C (dioxane); IR (KBr) (cm^{-1}): 3203 (NH), 2217 (CN), 1667, 1631(CO).^{1}H NMR (DMSO-d_6-D_2O) δ (ppm): 2.37 (s, 3H, CH_3), 7.33 (d, 2H, 4-CH_3-ph-$H_{3,5}$, J = 8 Hz), 7.50–7.60 (m, 3H, Ar-$H_{3,4,5}$), 7.76 (d, 2H, 4-CH_3-ph-$H_{2,6}$, J = 8 Hz), 7.90 (d, 2H, Ar-$H_{2,6}$), 9.47 (s, 1H, NH; exchangeable with D_2O), 10.47 (s, 1H, NH; exchangeable with D_2O), 10.68 (s, 1H, NH; exchangeable with D_2O); MS m/z (%): 345.32 (M^+, 15.12%), 60.20 (100%); Anal. Calcd for: $C_{19}H_{15}N_5O_2$ (345.35); (Found) C: 66.08, H: 4.38, N: 20.28; Found: C, 66.45; H, 4.49; N, 20.44%.

4.1.4.2. 4-chloro-N'-(5-cyano-1,6-dihydro-6-oxo-4-p-tolylpyrimidin-2-yl) benzohydrazide (4b). Yield 66%; yellow crystal; m.p. 315–318 °C (dioxane); IR (KBr) (cm^{-1}): 3254 (NH), 2218 (CN), 1662, 1634 (CO). ^{1}H NMR (DMSO-d_6-D_2O) δ (ppm): 2.37 (s, 3H, CH_3), 7.33 (d, 2H, 4-CH_3-ph-$H_{3,5}$, J = 7.6 Hz), 7.58 (d, 2H, 4-Cl-ph-$H_{3,5}$, J = 8 Hz), 7.76 (d, 2H, 4-CH_3-ph-$H_{2,4}$, J = 7.6 Hz), 7.94 (d, 2H, 4-Cl-ph-$H_{2,4}$, J = 8 Hz), 10.40 (s, 1H, NH; exchangeable with D_2O),10.72 (s,1H, NH; exchangeable with D_2O), 12.54 (s, 1H, NH; exchangeable with D_2O); MS m/z (%): 379.10 (M^+, 9.06%), 381.17 (M^+ + 2, 4.78), 139.02(100%); Anal. Calcd for: $C_{19}H_{14}ClN_5O_2$ (379.80), C, 60.09; H, 3.72; N, 18.44; Found: C, 59.87; H, 3.80; N, 18.78%.

4.1.4.3. N'-(5-cyano-1,6-dihydro-6-oxo-4-p-tolylpyrimidin-2-yl)-4-nitrobenzohy Drazide (4c). Yield 68%; yellow crystal; m.p. 334–336 °C (dioxane); IR (KBr) (cm^{-1}): 3241, 3111 (NH), 2222 (CN), 1688, 1650 (CO). ^{1}H NMR (DMSO-d_6-D_2O) δ (ppm): 2.38 (s, 3H, CH_3), 7.34 (d, 2H, 4-CH_3-ph-$H_{3,5}$, J = 8 Hz), 7.77 (d, 2H, 4-CH_3-ph-$H_{2,6}$, J = 8 Hz), 8.17 (d, 2H, 4-NO_2-ph-$H_{2,6}$, J = 8.4 Hz), 8.36 (d, 2H, 4-NO_2-ph-$H_{3,5}$, J = 8.4 Hz), 10.56 (s, 1H, NH; exchangeable with D_2O), 11.02 (s, 1H, NH; exchangeable with D_2O), 12.66 (s, 1H, NH; exchangeable with D_2O); MS (m/z): 390.08 (M^+, 12.63%), 44.05 (100%); Anal. Calcd for: $C_{19}H_{14}N_6O_4$ (390.35), C: 58.46, H: 3.61, N: 21.53; Found: C, 58.73; H, 3.67; N, 21.80%.

4.1.5. Synthesis of 1-(5-cyano-1,6-dihydro-6-oxo-4-p-tolylpyrimidin-2-yl)-4-phenylthiosemicarbazide (5)

A mixture of compound **2** (2.4 g, 10 mmol), phenyl isothiocyanate (1.2 g, 10 mmol) was refluxed in pyridine for 6 h. After cooling, the reaction mixture was poured on ice and neutralized with HCl. The solid separated was filtered, washed several times with cold water and re-crystallized from ethylacetate to give compound **5**.

Yield 90%; yellow crystal; m.p.130–132 °C (Ethylacetate); IR (KBr) (cm^{-1}): 3205 (NH), 2210 (CN), 1669 (CO). ^{1}H NMR (DMSO-d_6-D_2O) δ (ppm): 2.35 (s, 3H, CH_3), 6.89–7.32 (m, 5H, Ar-H), 7.46 (d, 2H, 4-CH_3-ph-$H_{3,5}$,J = 8 Hz), 7.52 (d, 2H, 4-CH_3-ph-$H_{2,6}$, J = 8 Hz), 9.73 (s, 3H, 3NH; exchangeable with D_2O), 9.80 (s, 1H, NH; exchangeable with D_2O); MS (m/z): 376.11 (M^+, 2.61%), 268.10 (100%); Anal. Calcd for: $C_{19}H_{16}N_6OS$ (376.43), C: 60.62, H: 4.28, N: 22.33; Found: C, 60.94; H, 4.39; N, 22.61%.

4.1.6. Synthesis of ethyl-N-(5-cyano-6-oxo-4-(p-tolyl)-1,6-dihydropyrimidin-2- yl)formohydrazonate (6)

A mixture of **2** (2.4 g, 10 mmole), triethylorthoformate (5 mL) and acetic anhydride (5 mL) was refluxed for 10 h., and allowed to cool and poured on ice. The obtained precipitate was filtered off, washed with H_2O, dried, and recrystallized from ethanol to give compound **6**.

Yield 76%; yellow crystal; m.p. 242–244 °C (EtOH); IR (KBr) (cm^{-1}): 3117 (NH), 2218 (CN), 1681 (CO); ^{1}H NMR (DMSO-d_6-D_2O) δ (ppm):1.39–1.42 (t, 3H, $OCH_2C\underline{H}_3$), 2.39 (s, 3H, CH_3), 4.30–4.32 (q, 2H,OCH_2), 7.37 (d, 2H, 4-CH_3-ph-$H_{3,5}$, J = 8 Hz), 7.80 (d, 2H, 4-CH_3-ph-$H_{2,6}$, J = 8 Hz), 9.39 (s, 1H, N = C$\underline{H}$); MS (m/z): 297.05 (M^+, 79%), 43.05 (100%); Anal. Calcd for: $C_{15}H_{15}N_5O_2$ (297.31), C: 60.60, H: 5.09, N: 23.56; Found: C, 60.87; H, 5.16; N, 23.38%.

4.1.7. Synthesis of N',N'-diacetyl-N-(5-cyano-4-ethoxy-6-p-tolyl pyrimidin-2-yl)acetohydrazide (7)

An equimolar amount of compound **2** and triethylorthoformate, was refluxed in acetic anhydride (10 mL) for 3 h. After standing, the crystals formed were filtered, and washed with ethanol to give compound **7**. X-ray crystallography was performed for the resultant crystals.

Yield 69%; yellow crystal; m.p.137–139 °C (EtOH); IR (KBr) (cm^{-1}): 2218 (CN), 1733, 1710 (CO);^{1}H NMR (DMSO-d_6-D_2O) δ (ppm): 1.34–1.38 (t, 3H, $OCH_2C\underline{H}_3$), 2.30 (s, 3H, $COCH_3$), 2.39 (s, 3H, CH_3), 2.76 (s, 6H, 2 $COCH_3$), 4.48–4.54 (q, 2H, CH_2), 7.40 (d, 2H, 4-CH_3-ph-$H_{3,5}$, J = 8 Hz), 7.84 (d, 2H, 4-CH_3-ph-$H_{2,6}$, J = 8 Hz); MS (m/z): 395.16 (M^+, 6.97%), 311.15 (100%); Anal. Calcd for: $C_{20}H_{21}N_5O_4$ (395.41), C: 60.75, H: 5.35, N: 17.71; Found: C, 60.49; H, 5.44; N, 18.06%.

4.1.8. Synthesis of N',N'-diacetyl-N-(5-cyano-1,6-dihydro-6-oxo-4-p-tolylpyrimidin-2-yl)acetohydrazide (8).

Compound **2** (10 mmol), in acetic anhydride (10 mL), was refluxed for 3 h. After cooling, the reaction mixture was poured on ice water to give a solid precipitate, which was filtered off, dried and recrystallized from ethanol to give compound **8**.

Yield 81%; yellow crystal; m.p.172–174 °C (EtOH); IR (KBr) (cm^{-1}): 3135 (NH), 2223 (CN), 1734, 1669 (CO). ^{1}H NMR (DMSO-d_6-D_2O) δ (ppm): 2.31 (s, 3H, $COCH_3$), 2.38 (s, 3H, CH_3), 2.64 (s, 6H, 2 $COCH_3$), 3.64 (s, 1H, NH; exchangeable with D_2O), 7.37(d, 2H, 4-CH_3-ph-$H_{3,5}$, J = 8 Hz), 7.79 (d, 2H, 4-CH_3-ph-$H_{2,6}$, J = 8 Hz); MS (m/z): 367.13 (M^+, 5.14%), 283.10 (100%); Anal. Calcd for: $C_{18}H_{17}N_5O_4$ (367.36), C: 58.85, H: 4.66, N: 19.06; Found: C, 59.16; H, 4.70; N, 19.31%.

4.1.9. Synthesis of 1,6-dihydro-2-(3,5-dimethyl-1H-pyrazol-1-yl)-6-oxo-4-p-tolylpyrimidine-5-carbonitrile (9)

A mixture of compound **2** (10 mmol) and acetylacetone (10 mmol) was refluxed in glacial acetic acid for 20 h. The reaction mixture was

cooled and poured on ice cold water. The formed precipitate was filtered, dried and recrystallized from ethanol afforded compound **9**.

Yield 56%; yellow crystal; m.p. 271–273 °C (EtOH); IR (KBr) (cm^{-1}): 3332 (NH), 2218 (CN), 1666 (CO). ^{1}H NMR (DMSO-d_6-D_2O) δ (ppm): 2.22 (s, 3H, CH_3), 2.38 (s, 3H, CH_3), 2.61 (s, 3H, CH_3), 6.29 (s, 1H, CH, pyrazole), 7.05 (d, 2H, 4-CH_3-ph-$H_{3,5}$, J = 8 Hz), 7.19 (d, 2H, 4-CH_3-ph-$H_{2,6}$, J = 8 Hz); MS (*m/z*): 305.17 (M^+, 100%); Anal. Calcd for: $C_{17}H_{15}N_5O$ (305.33), C: 66.87, H: 4.95, N: 22.94; Found: C, 66.72; H, 4.96; N, 23.28%.

4.1.10. Synthesis of 1,6-dihydro-2-(3-methyl-5-oxo-2H-pyrazol-1(5H)-yl)-6-oxo-4-p-tolylpyrimidine-5-carbonitrile (10)

A mixture of compound **2** (10 mmol), ethyl acetoacetate (10 mmol) in glacial acetic acid was refluxed for 12 h. The reaction mixture was cooled and poured on ice- water. The formed precipitate was filtered off, dried and recrystallized from ethanol to give compound **10**.

Yield: (68%); yellow crystal; m.p. 353–355 °C (EtOH); IR (KBr) (cm^{-1}): 3324 (NH), 2221(CN), 1746, 1665 (CO). ^{1}H NMR (DMSO-d_6-D_2O) δ (ppm): 2.30 (s, 3H, CH_3), 2.48 (s, 3H, CH_3), 4.31 (s, 1H, CH), 7.40 (d, 2H, 4-CH_3-ph-$H_{3,5}$, J = 8.4 Hz), 8.03 (d, 2H, 4-CH_3-ph-$H_{2,6}$, J = 8.4 Hz), 11.79 (s, 1H, NH; exchangeable with D_2O), 12.05 (s, 1H, NH; exchangeable with D_2O); MS (*m/z*): 307.00 (M^+, 27.35%), 76.98 (100%); Anal. Calcd for: $C_{16}H_{13}N_5O_2$ (307.31), Anal. Calcd for C: 62.53, H: 4.26, N: 22.79; Found: C, 62.79; H, 4.37; N, 23.12%.

4.1.11. Synthesis of 2-(1,3-dioxoisoindolin-2-ylamino)-1,6-dihydro-6-oxo-4-p-tolylpyrimidine-5-carbonitrile (11)

A mixture of compound **2** (10 mmol), and phthalic anhydride (10 mmol), was refluxed in glacial acetic acid (20 mL) for 12 h. The reaction mixture was cooled and poured on ice water. The formed precipitate was filtered, dried and recrystallized from ethanol.

Yield 73%; yellow crystal; m.p. 293–295 °C (EtOH); IR (KBr) (cm^{-1}): 3459 (NH), 2220 (CN), 1798, 1745, 1676 (CO). ^{1}H NMR (DMSO-d_6-D_2O) δ (ppm): 2.39 (s, 3H, CH_3), 7.36 (d, 2H, 4-CH_3-ph–$H_{3,5}$, J = 8 Hz), 7.54–7.68 (m, 2H, isoindolin-H), 7.74 (s, 1H, NH, D_2O exchangeable), 7.76 (s, 1H, NH, D_2O exchangeable), 7.80 (d, 2H, 4-CH_3-ph-$H_{2,6}$, J = 8 Hz), 7.92–8.00 (m, 2H, isoindolin-H); MS (*m/z*): 371.04 (M^+, 3.18%), 77.02 (100%); Anal. Calcd for: $C_{20}H_{13}N_5O_3$ (371.35), C: 64.69, H: 3.53, N: 18.86; Found: C, 64.99; H, 3.58; N, 19.09%.

4.1.12. Synthesis of 2-chloro-N'-(5-cyano-1,6-dihydro-6-oxo-4-p-tolylpyrimidin-2-yl) acetohydrazide (12)

A mixture of compound **2** (10 mmol), chloroacetyl chloride (10 mmol) was allowed to stir overnight at room temperature in dry dioxane (20 mL). The solid formed was filtered, dried and recrystallized from ethylacetate.

Yield 88%; yellow crystal; m.p. 260–262 °C (Ethyl acetate); IR (KBr) (cm^{-1}): 3292, 3140 (NH), 2222 (CN), 1711, 1661 (CO). ^{1}H NMR (DMSO-d_6-D_2O) δ (ppm): 2.36 (s, 3H, CH_3), 4.16 (s, 2H, CH_2), 7.32 (d, 2H, 4-CH_3-ph-$H_{3,5}$, J = 8 Hz), 7.74 (d, 2H, 4-CH_3-ph-$H_{2,6}$, J = 8 Hz), 10.48 (s, 1H, NH; exchangeable with D_2O), 12.35 (s, 1H, NH; exchangeable with D_2O); MS (*m/z*): 317.10 (M^+, 8.57%), 319.10 (M^+ + 2, 2.76%), 118.09 (100%); Anal. Calcd for: $C_{14}H_{12}ClN_5O_2$ (317.73): C, 52.92; H, 3.81, N: 22.04; Found: C, 53.17; H, 3.89; N, 22.37%.

4.1.12.1. X-ray crystallography. X-ray structure of the compound **7** was performed in the Central service and x-ray laboratories, National Research Centre, Cairo, Egypt. Crystal and molecular structures prepared by Maxus Computer Program for the Solution and Refinement of crystal structures. All diagrams and calculations were performed maX us (Bruker Nonius, Delft & Mac Science, Japan) (Fig. 7). Extinction correction: none. Atomic scattering factors from Waasmaier & Kirfel, 1995. Data collection: Kappa CCD 1522302. Cell refinement: HKL. Scalepack and Data reduction: Denzo. Program(s) used to solve structure: DIRDIF. Program (s) used to refine structure: SHELXL-97, Molecular graphics: ORTEP, software used to prepare material for publication: maXus [30–34].

4.2. Biological evaluation

4.2.1. In vitro anticancer activity

Three human cancer cell lines, namely hepatocellular carcinoma (HePG-2), mammary gland (MCF-7) and colorectal carcinoma (HCT-116), are used to determine in vitro the anticancer activity of the synthesized compounds. The tested cell lines were supplied from the US National Cancer Institute. The reported standard procedure [35] was utilized as follows. The tested cells were plated in 96-well microplates; the total volume per well was adjusted at 100 µL. Then, incubation of cells was performed at 37 °C, 5% CO_2, 95% air and 100% relative humidity for 24 h before addition of synthesized compounds. After 24 h, only two plates of each cell line were selected and fixed in situ with TCA, in order to exemplify a measurement of the cell population for each cell line during drug application. The title compounds and fluorouracil, the reference drug, were dissolved in DMSO at 400-fold the desired final maximum test concentration and stored at freezing point prior to use. During addition of drug, the frozen concentrate was dissolved and diluted to twice the desired final maximum test concentration with gentamicin solution (50 mg/mL). To reach the desired final drug concentrations, different tested compound dilutions (100 mL) were added to the appropriate microtiter wells containing 100 mL of medium. The tested compounds as well as 5-fluorouracil as reference drug were added. Then, the plates were incubated for an additional 48 h at 37 °C, 5% CO_2, 95% air and 100% relative humidity. The assay was terminated by addition of cold TCA for adherent cells followed by incubation for 60 min at 4 °C. The supernatant was removed, and the plates were washed five times with excessive water and dried. A solution of 0.4% (w/v) sulforhodamine B (100 mL) in 1% acetic acid was added to each well, followed by incubation at room temperature for 10 min. After staining, the plates were washed with 1% acetic acid to remove unbound dye and air-dried. Bound stain was dissolved with 10 mM Trizma base. Spectrophotometric assay of the optical density (OD) of each well was determined at 564 nm with an ELISA microplate reader (ChroMate-4300, FL, USA). Boltzmann sigmoidal concentration response curvewas used to calculate the IC_{50} values through the nonlinear regression fitting models (GraphPad Prism, version 5). The means of three separate experiments was reported as final result. ANOVA test was used to analyze the statistical differences, wherein the differences were considered to be significant at $p < 0.05$.

4.2.2. In vitro assay of thymidylate synthase (TS) activity

The activity of TS was measured spectrophotometrically at pH 7.4 and 30 °C in a mixture containing 0.1 M 2-mercaptoethanol, 0.0003 M (6R,S)-tetrahydrofolate, 0.02 M MgCl2, 0.012 M formaldehyde, 0.04 M TrisHCl, 0.001 M dUMP and 0.00075 M Na EDTA according to the reported procedure [23]. In general, to initiate the reaction, the enzyme was added in the absence of inhibitor producing a change in absorbance at 340 nm of 0.016/min. Then, four inhibitor concentrations were used to determine the percent inhibition. Next, concentration–inhibition response curve for the test compounds was generated to determine median inhibitory concentration (IC_{50}). The obtained data were compared with 5-fluorouracil as a standard TS inhibitor. The standard deviations for determination of the 50% points were within ± 10% of the values given.

HT.S enzyme used to perform the kinetic assays was obtained from Sigma Co., St. Louis, USA, via Holding company for biological products and vaccines (VACSERA), Cairo, Egypt.

4.2.3. Determination of the active caspase-3

To determine the effect of the synthesized compounds on apoptosis, the active caspase-3 level was measured by using Quantikine-Human active Caspase-3 Immunoassay (R&D Systems, Inc. Minneapolis, USA)

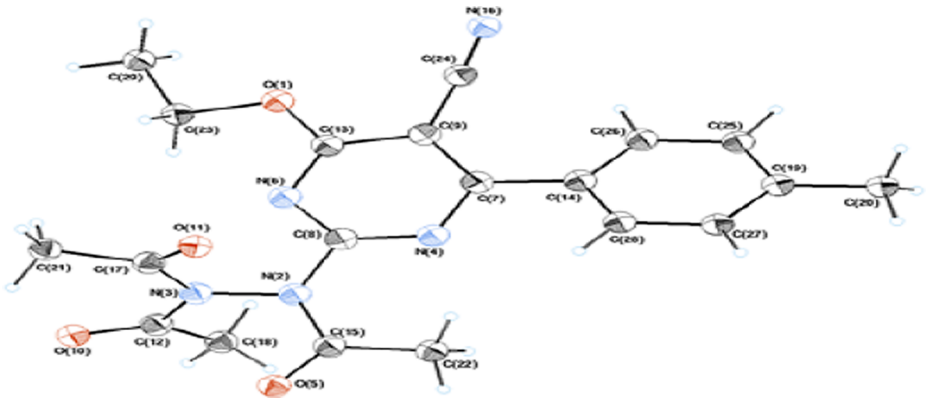

Fig. 7. ORTEP drawing of the molecule **7**.

according to the manufacturer protocol. Briefly, after washing the cells with PBS, the cells were collected and lysed by adding it to the extraction buffer containing protease inhibitors (1 mL per 1–107 cells.) then the lysate was diluted immediately prior to the assay. At the end of the assay the optical density of each well was determined within 30 min using a microplate reader set at 450 nm.

4.2.4. RNA extraction, real time PCR analysis and quantification of gene expression

The gene expression of Bax and Bcl-2 was assessed by total RNA extraction from cells using RNeasy Mini Kit® (Qiagen Inc. Valencia, CA, USA). cDNA library was constructed from different treatments using High-Capacity cDNA Reverse Transcription Kit (Applied Biosystems, Foster City, CA). The archived cDNA libraries were then subjected to quantitative real time PCR reactions [36] using cyber green fluorophore (Fermentas Inc., Glen Burnie, MD, USA).

4.3. Molecular docking

The docking simulation studies were performed using Molecular Operating Environment (MOE®) version 2014, 0901 Chemical Computing Group Inc., Montreal, Canada. The X-ray crystallographic structure hTS (code 6QXG) was obtained from the Protein Data Bank through the internet. The enzyme was prepared for docking studies by: The ligand and water molecules were removed from hTS active site. Hydrogen atoms were added to the system with their standard geometry. The atoms connection and type were checked for any errors with automatic correction. Selection of the receptor and its atoms potential were fixed. MOE Alpha Site Finder was used for the active site search in the enzyme structure using all default items. Dummy atoms were created from the obtained alpha Spheres. The following methodology was applied: The enzyme active site file was loaded and the Dock tool was initiated. The program specifications were adjusted to: Dummy atoms as the docking site. Triangle matcher as the placement methodology to be used. London dG as Scoring methodology to be used and was adjusted to its default values. The MDB file of the ligand to be docked was loaded and Dock calculations were run automatically. The obtained poses were studied and the poses showed best ligand-enzyme interactions were selected and stored for energy calculations. The docking scores were expressed in negative energy terms; the lower the binding free energy, the better the binding affinity. The structures of ligands were drawn in Chem Draw Ultra 8.0 (Cheminformatics Software company based in Cambridge, Massachusetts, USA) and saved as mol. The two-dimensional structure of the selected compounds was converted into their three-dimensional form and energy minimized using the MMFF94x force field until a root-mean-square deviation of atomic position gradient of 0.01 Kcal/mol/E was reached.

Declaration of Competing Interest

The authors declare no conflict of interest, financial or otherwise.

Acknowledgements

Authors are thankful to the scientific research team of VASERA CO., Giza, Egypt, for providing laboratory facilities for biological activity.

Appendix A. Supplementary material

Supplementary data to this article can be found online at https://doi.org/10.1016/j.bioorg.2019.103159.

References

[1] G.L. Patrick, An Introduction to Medicinal Chemistry, fourth ed., Oxford University Press Inc., New York, 2009.
[2] M.A. Khan, H. Chen, M. Tania, D. Zhang, Anticancer activities of Nigella Sativa (Black Cumin), Afr. J. Tradit. Complement Altern. Med. 8 (2011) 226–232.
[3] Y. Zhou, Y. Li, T. Zhou, J. Zheng, S. Li, H. Li, Dietary natural products for prevention and treatment of liver cancer, Nutrients 8 (2016) 156–178.
[4] K.I. Deen, H. Silva, R. Deen, P.C. Chandrasinghe, Colorectal cancer in the young, many questions, few answers, World. J. Gastrointest. Oncol. 8 (2016) 481–488.
[5] C. Avendano, J.C. Menendez, Medicinal Chemistry of Anticancer Drugs, first ed., Elsevier B. V, Oxford, UK, 2008.
[6] R. Dudhe, P.K. Sharma, P. Verma, A. Chaudhary, Pyrimidine as anticancer agent: A review, J. Adv. Sci. Res. 2 (2011) 10–17.
[7] S.I. Szafraniec, K.J. Stachnik, J.S. Skierski, New nucleoside analogs in the treatment of hematological disorders, Acta Pol. Pharm. 61 (2004) 223–232.
[8] Y.M. Choi, H.K. Yeo, Y.W. Park, J.Y. Lee, Structural analysis of thymidylate synthase from Kaposi's sarcoma-associated herpes virus with the anticancer drug raltitrexed, PLoS ONE 11 (2016) 1–12.
[9] D.B. Longley, D.P. Harkin, P.G. Johnston, 5-Fluorouracil: mechanism of action and clinical strategies, Nat. Rev. Cancer 3 (2003) 330–338.
[10] M.P. Costi, S. Ferrari, A. Venturelli, S. Calò, D. Tondi, D. Barlocco, Thymidylate synthase structure, function and implication in drug discovery, Curr. Med. Chem. 12 (2005) 763–771.
[11] D. Chen, A. Jansson, D. Sim, A. Larsson, P. Nordlund, Structural analyses of human thymidylate synthase reveal a site that may control conformational switching between active and inactive states, J. Biol. Chem. 292 (2017) 13449–13458.
[12] H. Backus, D. Wouters, C. Ferreira, V.V. Houten, R. Brakenhoff, H. Pinedo, G. Peters, Thymidylate synthase inhibition triggers apoptosis via caspases-8 and-9 in both wild-type and mutant p53 colon cancer cell lines, Eur. J. Cancer 39 (2003) 1310–1317.
[13] S. Chang, C. Lin, R. Lee, F. Chang, S. Lee, S. Yem, Y. Chao, Calcification of liver metastases in a colon cancer patient following chemotherapy with 5-fluorouracil: A case report, Chin. J. Radiol. 27 (2002) 73–77.
[14] W. Ichikawa, Prediction of clinical outcome of fluoropyrimidine-based chemotherapy for gastric cancer patients, in terms of the 5-fluorouracil metabolic pathway, Gastric Cancer 9 (3) (2006) 145–155.
[15] L. Taddia, D. D'Arca, S. Ferrari, C. Marraccini, L. Severi, G. Ponterini, Y.G. Assaraf, G. Marverti, M.P. Costi, Inside the biochemical pathways of thymidylate synthase perturbed by anticancer drugs: Novel strategies to overcome cancer chemoresistance, Drug Resist. Updat. 23 (2015) 20–54.
[16] J. Wang, L. Peng, R. Zhang, Z. Zheng, C. Chen, K.L. Cheung, M. Cui, G. Bian, F. Xu, D. Chiang, Y. Hu, Y. Chen, G. Lu, J. Yang, H. Zhang, J. Yang, H. Zhu, S. Chen, K. Liu, M. Zhou, A.G. Sikora, L. Li, B. Jiang, H. Xiong, 5-Fluorouracil targets thymidylate synthase in the selective suppression of TH17 cell differentiation, Oncotarget. 7

(2016) 19312–19326.
[17] M.I. El-Zahar, S.S. Abd El-Karim, M.E. Haiba, M.A. Khedr, Synthesis antitumor activity and molecular docking study of novel benzofuran-2-yl pyrazole pyrimidine derivatives, Acta Pol. Pharm. 68 (2011) 357–373.
[18] M.M. Mohamed, A.K. Khalil, E.M. Abbass, A.M. El-Naggar, Design, synthesis of new pyrimidine derivatives as anticancer and antimicrobial agents, Synth. Commun. 47 (2017) 1441–1457.
[19] S.A. Rizk, A.M. El-Naggar, A.A. El-Badawy, Synthesis, spectroscopic characterization and computational chemical study of 5-cyano-2-thiouracil derivatives as potential antimicrobial agents, J. Mol. Struct. 1155 (2018) 720–733.
[20] A.M. El-Naggar, M.M. Abou-El-Regal, S.A. El-Metwally, F.F. Sherbiny, I.H. Eissa, Synthesis characterization and molecular docking studies of thiouracil derivatives as potent thymidylate synthase inhibitors and potential anticancer agents, Mol. Diversity 21 (2017) 967–983.
[21] C. Rami, L. Patel, C.N. Patel, J.P. Parmar, Synthesis, antifungal activity, and QSAR studies of 1, 6-dihydropyrimidine derivatives, J. Pharm. Bioall. Sci. 5 (2013) 277–289.
[22] A.M. Hamouda, Synthesis of novel pyrimidines thiazolopyrimidines, triazolopyrimidines and pyrimidotriazines as potent antimicrobial agent, Der. Pharma. Chem. 6 (2014) 346–357.
[23] A.J. Wahba, M. Friedkin, The enzymatic synthesis of thymidylate i Early steps in the purification of thymidylate synthetase of Escherichia coli, J. Biol. Chem. 237 (1962) 3794–3801.
[24] E. Galvani, G.J. Peters, E. Giovannetti, Thymidylate synthase inhibitors for non-small cell lung cancer, Expert Opin. Investig. Drugs 20 (2011) 1343–1356.
[25] P. Ceppi, I. Rapa, M.L. Iacono, L. Righi, J. Giorcelli, M. Pautasso, A. Bille', F. Ardissone, M. Papotti, G.V. Scagliotti, Expression and pharmacological inhibition of thymidylate synthase and Src kinase in nonsmall cell lung cancer, Int. J. Cancer 130 (2012) 1777–1786.
[26] L.M. Gibson, L.R. Celeste, L.L. Lovelace, L. Lebioda, Acta Crystallogr. D Biol. Crystallogr. 67 (2011) 60–66.
[27] S.V. Tiwari, J.A. Seijas, M.P. Vazquez-Tato, A.P. Sarkate, D.K. Lokwani, A.P.G. Nikalje, Ultrasound mediated one-Pot, three component synthesis, docking and ADME prediction of novel 5- amino-2-(4-chlorophenyl)-7-substituted phenyl-8,8a-dihydro-7H-(1,3,4)thiadiazolo(3,2-α)pyrimidine-6-carbonitrile derivatives as anticancer agents, Molecules 21 (2016) 894–906.
[28] A.F. Eweas, Q.M.A. Abdallah, E.S.I. Hassan, Design, synthesis, molecular docking of new thiopyrimidine-5-carbonitrile derivatives and their cytotoxic activity against HepG2 cell line, J. Appl. Pharm. Sci. 4 (2014) 102–111.
[29] Y.L.N. Murthy, R.M.R. Saviri, A.R. Parimi, S. Nareesh, Mg(OMe)2 as a versatile catalyst for one-pot synthesis of 6-aryl-5-cyano-2- (oxo / thio) uracil derivatives and their antimicrobial evaluations, Org. Commun. 6 (2013) 47–54.
[30] S. Mackay, C. J.Gilmore, C. Edwards, N. Stewart, K. Shankland, maXus Computer Program for the Solution and Refinement of Crystal Structures, Bruker Nonius, The Netherlands, MacScience, Japan & The University of Glasgow, 1999.
[31] C.K. Johnson, ORTEP–II. A Fortran Thermal–Ellipsoid Plot Program. Report ORNL-5138, Oak Ridge National Laboratory, Oak Ridge, Tennessee, USA, 1976.
[32] P.T. Beurskens, G. Beurskens, W.P. Bosman, R.S. de Gelder, S. Garćia–Granda, R.O. Gould, J.M.M. Smits, The DIRDIF96 program system, Technical Report of the Crystallography Laboratory, University of Nijmegen, The Netherlands,1996.
[33] G.M. Sheldrick, SHELXL97. Program for the Refinement of Crystal Structures, University of Gottingen, Germany, 1997.
[34] R.H. Blessing, An empirical correction for absorption anisotropy, Acta Cryst. A 51 (1995) 33–38.
[35] P. Skehan, R. Storeng, D. Scudiero, A. Monks, J. Mcmahon, D. Vistica, J.T. Warren, H. Bokesch, S. Kenney, M.R. Boyd, New colorimetric cytotoxicity assay for anticancer-drug screening, J. Natl. Cancer Inst. 82 (1990) 1107–1112.
[36] M.C. Longo, M.S. Berninger, J.L. Hartley, Use of uracil DNA glycosylase to control carry-over contamination in polymerase chain reactions, Gene 93 (1990) 125–128.